ROTATIONALLY INVARIANT QUADRATURES FOR THE SPHERE

CORY AHRENS AND GREGORY BEYLKIN

Abstract. We construct nearly optimal quadratures for the sphere that are invariant under the icosahedral rotation group. These quadratures integrate all $(N+1)^2$ linearly independent functions in a rotationally invariant subspace of maximal order and degree N. The nodes of these quadratures are nearly uniformly distributed and the number of nodes is only marginally more than the optimal $(N+1)^2/3$ nodes. Using these quadratures, we discretize the reproducing kernel on a rotationally invariant subspace to construct an analogue of Lagrange interpolation on the sphere. This representation uses function values at the quadrature nodes. In addition, the representation yields an expansion that uses a single function centered and mostly concentrated at nodes of the quadrature, thus providing a much better localization than spherical harmonic expansions. We show that this representation may be localized even further. We also describe two algorithms of complexity $\mathcal{O}(N^3)$ for using these grids and representations. Finally, we note that our approach is also applicable to other discrete rotation groups.

1. Introduction

Many problems in physics, mathematics and engineering involve integration and interpolation on the sphere in $\mathbb{R}^3$. Of particular importance are discretizations of rotationally invariant subspaces of $L^2\left(\mathbb{S}^2\right)$ that integrate all spherical harmonics up to a fixed order and degree. A typical approach to discretizing the sphere is that of equally spaced discretization in azimuthal angle and Gauss-Legendre discretization in polar angle, leading to an unreasonably dense concentration of nodes near the poles. It is well known that in a variety of applications such concentration of nodes may lead to problems when using these grids.

Alternatively, Sobolev [39] (see also [31, 40]) suggested the use of grids that are invariant under finite rotation groups. In such constructions there is no clustering of nodes and, moreover, the number of nodes necessary to integrate a particular subspace is close to optimal. In fact, in some cases it is optimal, a notion we make precise later. There have been several constructions of this type of grids using algebraic approaches (see [34, 26, 27, 31]

This research was partially supported by AFOSR grant FA9550-07-1-0135, NSF grant DMS-0612358, DOE/ORNL grants 4000038129 and DE-FG02-03ER25583.
http://dx.doi.org/10.1098/rspa.2009.0104 Proc. R. Soc. A 465, 3103-3125, 2009 .

and references therein) but the technique limits the results to a few particular orders and degrees. An attempt to construct grids invariant under the icosahedral group may be found in [23, 22] (with some negative weights in the early construction). We also refer to [7, 42] for a review and further references.

In this paper we develop a systematic numerical approach for constructing nearly optimal quadratures invariant under the icosahedral group to integrate rotationally invariant subspaces of $L^2\left(\mathbb{S}^2\right)$ up to a fixed order and degree. Using these grids and a reproducing kernel, we show how to replace the standard basis of spherical harmonics on a rotationally invariant subspace by a representation formed using a single function centered at the quadrature nodes. The reproducing kernel is mostly concentrated near the corresponding grid point. In the resulting representation, the coefficients, up to a factor, are the values on the grid of the function being represented. We may interpret this construction as an analogue of Lagrange interpolation on the sphere (see also [36, 37]) and note that it allows us to develop well conditioned linear systems for interpolation in contrast to some earlier constructions [10, 11].

An alternative to spherical harmonics has long been sought, especially for numerical purposes. Spherical harmonics provide an efficient orthonormal basis, nicely subdivided into rotationally invariant subspaces. However, the global support of these functions poses a serious difficulty in problems where physical effects are localized. In fact, the global nature of spherical harmonics is a consequence of their optimality. Therefore, if we want localized functions to represent the same subspaces, we necessarily must have a less efficient representation.

Work on alternative representations has accelerated since the development of wavelets. Several proposals for local and multiresolution representations have been suggested over the years, resulting in numerous publications (see e.g. [12, 43, 4, 15] and references therein). Several attempts to generalize the wavelet transform on Euclidean spaces to the sphere have been made (see e.g. [19, 20, 1, 12] and references therein). One particular generalization [1] uses a doubly periodic discretization of the sphere to provide algorithmic efficiency. Such discretization, however, does not assure rotational invariance as the nodes will necessarily concentrate near the polar regions. Discrete multiresolution transforms on the sphere have been suggested using geodesic grids [35], equal area subdivisions [29] and irregular grids in [8, 25], mostly for the purpose of graphics. These transforms are also useful for the analysis of data measured on the sphere, e.g., for geophysical or astrophysical applications. Such transforms may have a formal extension to high order versions, but only low order constructions appear to be practical.

A practical high order local construction based on a "cubed sphere" has been successfully used in global atmospheric modeling [43] and geodesy [4].

As a replacement for spherical harmonics, such "cubed sphere" representations proved to be practical in the development of high order numerical techniques but, at the same time, they lack a number of useful properties.

We view our approach as the first step in constructing a local and multiresolution representation of functions on the sphere that respects rotationally invariant subspaces. We note that the high efficiency of quadratures constructed in this paper implies a near uniform distribution of nodes on the sphere. On the other hand, the nodes maintain a regular organization visually similar to that of geodesic or equal area grids. Moreover, our grids are associated with rotationally invariant subspaces, an important property in a number of numerical applications, e.g., geodesy. To date, we have constructed grids which integrate subspaces of maximum order and degree ranging from 5 up to 210. As an example, we illustrate in Figure 3.2 a grid with 7212 nodes integrating subspaces of maximal order and degree 145.

Our method for constructing these grids is based on Newton's method and, hence, the key to its success is a good initial distribution of nodes. At first, as the initial distribution we used spherical codes with icosahedral symmetry constructed by Hardin, Sloane and Smith [16]. We then developed a simple approach to map a two dimensional lattice to the icosahedron and then to the sphere yielding the initial distribution of nodes structurally similar to that of the resulting quadrature nodes. We describe this approach in Section 3.3.

The rotationally invariant spherical grids constructed here have many applications. Let us mention a few specific problems in some detail. First, due to the central role played by spherical harmonics in the theory of gravity and magnetic fields, solutions to many geodetic problems use them as a basis (see, e.g., [2, 18]). Yet, their global support is inconsistent with the physical nature of the problem leading to many difficulties in, e.g., constructing gravity models. The grids developed in this paper provide a first step toward replacing spherical harmonics with localized functions. We plan to continue work in this direction. Second, the equations used in global atmospheric modeling are typically posed on the sphere [44]. Current spectral methods which use spherical harmonics suffer from the above mentioned problems of nodal clustering and require additional steps to alleviate the problem [21]. An approach in [43] provides a practical alternative but also introduces artificial singularities associated with vertices of the cube. The new representations developed in this paper eliminate clustering and singularities due to the coordinate system and should provide efficient solution methods. Third, acoustic and electromagnetic scattering problems posed as integral equations involve integration over spherical domains [5]. New algorithms for the numerical solution of these integral equations may be based on the results of this paper. Finally, we mention a numerical technique used in molecular dynamics calculations known as discrete variable representation (DVR) [30]. In the DVR method, integrals over spherical domains in $\mathbb{R}^3$ are

computed and some implementations of the DVR method [17] use quadratures developed by Lebedev [26, 27]. Our quadratures should extend such methods by allowing effectively an arbitrary order and degree.

We start by reviewing necessary mathematics, outline a general method for constructing nodes invariant under the icosahedral group and illustrate resulting quadratures through several examples. Based on these new quadratures, we also develop a representation of functions in rotationally invariant subspaces as linear combinations of a single function centered at the quadrature nodes. We then discuss properties of this representation which may be interpreted as an analogue on the sphere of the usual Lagrange interpolation. We present two $\mathcal{O}\left(N^3\right)$ algorithms to work with these new grids (here N is the maximum order and degree of the subspace). We also consider a representation via localized functions and briefly describe its properties. We conclude by listing directions for future research in developing practical methods for applications dealing with the sphere.

2. Preliminaries

Here we establish notation and state some well known results about spherical harmonics, reproducing kernels and quaternionic representation of rotations. We also formulate two theorems of Sobolev [39] for quadratures that are invariant under a finite rotation group and a theorem of Molien [33] on the number of invariants for a finite group.

2.1. **Spherical harmonics and reproducing kernels.**

We denote the sphere in $\mathbb{R}^3$ as $\mathbb{S}^2 = \left\{\mathbf{x} \in \mathbb{R}^3 : x^2 + y^2 + z^2 = 1\right\}$. An orthonormal basis for $L^2\left(\mathbb{S}^2\right)$ is given by the spherical harmonics,

$$Y_n^m(\theta,\phi) = \frac{1}{\sqrt{2\pi}} \overline{P}_n^m(\cos\theta)\, e^{im\phi},\ 0 \le |m| \le n, \quad n = 0, 1, \ldots, \tag{2.1}$$

where the polar angle $\theta \in [0,\pi]$, the azimuthal angle $\phi \in [0, 2\pi)$ and $\overline{P}_n^m$ are the normalized associated Legendre functions,

$$\overline{P}_n^m(\mu) = (-1)^m \sqrt{\frac{(2n+1)\,(n-m)!}{2\,(n+m)!}} \frac{\left(1-\mu^2\right)^{m/2}}{2^n n!} \frac{d^{n+m}}{d\mu^{n+m}} \left(\mu^2 - 1\right)^n, \ \ |\mu| \le 1.$$

Any $f \in L^2\left(\mathbb{S}^2\right)$ may be expanded as

$$f(\theta,\phi) = \sum_{n=0}^{\infty} \sum_{m=-n}^{n} c_{nm} Y_n^m(\theta,\phi), \tag{2.2}$$

with the coefficients given by

$$c_{nm} \equiv \langle f, Y_n^m \rangle = \int_{\mathbb{S}^2} f(\theta,\phi)\, Y_n^{*m}(\theta,\phi)\, d\Omega, \tag{2.3}$$

where $\langle \cdot, \cdot \rangle$ is the inner product and * denotes complex conjugation. We define a subspace of spherical harmonics with fixed degree n as

$$\mathcal{H}_n = \operatorname{span}\left\{Y_n^m(\theta,\phi),\ |m| \le n\right\}. \tag{2.4}$$

The spherical harmonics Y_n^m are linearly independent and, hence, the dimension of $\mathcal{H}_n$ is $2n+1$. The subspace of maximum degree N is then the direct sum

$$\mathcal{P}_N = \bigoplus_{n=0}^{N} \mathcal{H}_n = \operatorname{span}\left\{Y_n^m(\theta,\phi),\ |m| \le n,\ 0 \le n \le N\right\} \tag{2.5}$$

and has dimension $(N+1)^2$. We make use of the addition theorem (see e.g. [13]), which states that for $\boldsymbol{\omega}, \boldsymbol{\omega}' \in \mathbb{S}^2$

$$\frac{2n+1}{4\pi} P_n\left(\boldsymbol{\omega}\cdot\boldsymbol{\omega}'\right) = \sum_{m=-n}^{n} Y_n^m(\boldsymbol{\omega})\, Y_n^{*m}\left(\boldsymbol{\omega}'\right), \tag{2.6}$$

where P_n is the Legendre polynomial of degree n. We also use the reproducing kernel for $\mathcal{P}_N$ which satisfies

$$f(\boldsymbol{\omega}) = \int_{\mathbb{S}^2} K\left(\boldsymbol{\omega}\cdot\boldsymbol{\omega}'\right) f\left(\boldsymbol{\omega}'\right) d\Omega', \quad f \in \mathcal{P}_N, \tag{2.7}$$

where

$$K\left(\boldsymbol{\omega}\cdot\boldsymbol{\omega}'\right) \equiv \sum_{n=0}^{N} \frac{2n+1}{4\pi} P_n\left(\boldsymbol{\omega}\cdot\boldsymbol{\omega}'\right). \tag{2.8}$$

The identity in (2.7) may be verified by using (2.6). We rely on (2.7) to develop a new representation of functions in $\mathcal{P}_N$ and an analogue of Lagrange interpolation on the sphere.

2.2. ***Quaternionic representation of rotations and points on the sphere.*** We use quaternions to represent points on the sphere as well as perform rotations. A quaternion $\mathbf{q}$ is defined as

$$\mathbf{q} = w + \mathbf{i}x + \mathbf{j}y + \mathbf{k}z,$$

where $w, x, y, z \in \mathbb{R}$ and the symbols $\mathbf{i}$, $\mathbf{j}$, $\mathbf{k}$ satisfy $\mathbf{i}^2 = \mathbf{j}^2 = \mathbf{k}^2 = \mathbf{ijk} \equiv -1$ and $\mathbf{ij} = \mathbf{k}$, $\mathbf{jk} = \mathbf{i}$, $\mathbf{ki} = \mathbf{j}$. Here w is the scalar part of the quaternion and (x, y, z) is its vector part, which may be associated with a vector in $\mathbb{R}^3$. Thus, vectors in $\mathbb{R}^3$ may be represented by quaternions by simply setting the scalar part to zero. The norm of $\mathbf{q}$ is defined as

$$\|\mathbf{q}\| = \left(w^2 + x^2 + y^2 + z^2\right)^{.1/2}$$

Quaternions form an algebra, $\mathbb{H}$, and the multiplicative inverse of $\mathbf{q}$ is given by

$$\mathbf{q}^{-1} = (w + \mathbf{i}x + \mathbf{j}y + \mathbf{k}z)^{-1} = \frac{w - \mathbf{i}x - \mathbf{j}y - \mathbf{k}z}{\|\mathbf{q}\|^2}.$$

We represent points on the sphere as quaternions with zero scalar part and unit norm, $\mathbf{q} \in \mathbb{H}$, $\|\mathbf{q}\| = 1$.

In order to rotate a point on the sphere represented by $\mathbf{v} \in \mathbb{H}$ by an angle θ around the unit vector $\mathbf{u} \in \mathbb{R}^3$, we construct the quaternion, $\mathbf{q_r} \in \mathbb{H}$,

$$\mathbf{q_r} = \cos\left(\frac{\theta}{2}\right) + \sin\left(\frac{\theta}{2}\right)\mathbf{u}.$$

The rotated point is given by the quaternion $\mathbf{v}' = \mathbf{q_r}\mathbf{v}\mathbf{q_r}^{-1}$ and it is not difficult to show that $\mathbf{v}'$ has zero scalar part and unit norm (see e.g. [24]). We use quaternions to represent actions of the icosahedral group[1].

2.3. **Sobolev's theorems.** Sobolev's paper [39] contains two key results that we now summarize. For clarity, we specialize these results to the case of the icosahedral rotation group noting that our approach may be applied without essential modifications to other discrete rotation groups.

Consider evaluating the integral $\int_{\mathbb{S}^2} f(\theta,\phi)\, d\Omega$, where f belongs to the rotationally invariant subspace $\mathcal{P}_N$, using a quadrature rule with nodes $\{\theta_i,\phi_i\}_{i=1}^M$ and weights $\{w_i\}_{i=1}^M$ so that

$$\int_{\mathbb{S}^2} f(\theta,\phi)\, d\Omega = \sum_{i=1}^{M} w_i f(\theta_i,\phi_i) \equiv Q(f)$$

for all $f \in \mathcal{P}_N$. Since both the integration domain and the subspace have rotational symmetry, is it natural to look for rotationally invariant quadrature rules. Following [39], we define invariant quadrature rules as follows: given a finite rotation group G, a quadrature rule Q is invariant under G if for all $g \in G$,

$$\sum_{i=1}^{M} w_i f\left(g^{-1}\theta_i, g^{-1}\phi_i\right) = \sum_{i=1}^{M} w_i f(\theta_i,\phi_i).$$

We have

Theorem 2.1. *Let Q be a quadrature rule invariant under the group G. Then Q is exact for all functions $f \in \mathcal{P}_N$ if and only if Q is exact for functions f invariant under G.*

This theorem effectively reduces the size of the system of nonlinear equations which must be solved to determine a quadrature invariant under the group G. The next result gives a formula to calculate the number of invariant functions under the group G in a subspace of spherical harmonics $\mathcal{H}_n$ of a given degree n. Let $q_1 = 5$ be the number of edges meeting at a vertex of an icosahedron, $q_2 = 3$ be the number of sides of its (triangular) face and $q_3 = 2$ denote the order of rotation about mid-points of opposing edges.

Theorem 2.2. *For a given degree n, the number of functions invariant under the icosahedral rotation group in a subspace of spherical harmonics $\mathcal{H}_n$ is given by*

$$S(n) = \left\lfloor \frac{n}{q_1} \right\rfloor + \left\lfloor \frac{n}{q_2} \right\rfloor + \left\lfloor \frac{n}{q_3} \right\rfloor - n + 1,$$

[1]See online supplement http://please-insert-address

where $\lfloor\,\rfloor$ *denotes the integer part*[2].

This result may also be obtained using a theorem of Molien (circa 1897) [33]. In his approach the number of invariants for a finite group may be obtained as coefficients of a generating function. In our case we have (see [32])

Theorem 2.3. *For a given degree* n*, the number of functions invariant under the icosahedral rotation group in a subspace of spherical harmonics* $\mathcal{H}_n$ *is given by coefficients* $S(n)$ *of the series expansion of the generating function,*

$$\frac{1+t^{15}}{(1-t^6)(1-t^{10})} = \sum_{n=0}^{\infty} S(n)t^n.$$

It is not difficult to see that both Theorems 2.2 and 2.3 yield the same result. We use theorems of this section to determine the number of equations contributed by each subspace $\mathcal{H}_n$ to the nonlinear system of equations determining the quadrature nodes and weights.

3. Quadratures for the sphere

The main difficulty in constructing quadratures comes from the need to solve a large system of nonlinear equations. Without using special structure of these equations, general root finding or optimization methods typically fail. The essence of our approach is to develop and use such structure within a root finding method.

We start by noting four different types of orbits of the icosahedral rotation group. In general, with three exceptions described below, a point on the sphere under the action of the group generates a total of 60 points (which is the group's order). However, if a point is a vertex of the icosahedron, then it generates a total of only 12 distinct points. Also, if a point is the projection of the center of an icosahedron face onto the sphere, it generates 20 distinct points in total. Finally, if a point is the projection onto the sphere of the mid-point of an edge, it generates a total of 30 distinct points. When describing these different types of orbits it is sufficient to consider a single point, a generator of its orbit. The orbit of a point with spherical coordinates (θ, ϕ) is the set $\left\{\left(g_i^{-1}\theta, g_i^{-1}\phi\right) \mid g_i \in G\right\}$ and, depending on the type of orbit, has cardinality 12, 20, 30 or 60.

With these types of orbits in mind, we consider four types of quadratures. The first type assumes that all generators, except for a vertex of the icosahedron, give rise to orbits of size 60, i.e.,

$$Q_v(f) = w_v \sum_{i=1}^{12} f\left(\theta_i^v, \phi_i^v\right) + \sum_{j=1}^{N_g} w_j \sum_{i=1}^{60} f\left(\theta_i^{(j)}, \phi_i^{(j)}\right), \tag{3.1}$$

[2]We note that an alternative formula for $S(n)$, Eq.17 in Sobolev's paper [39], is incorrect but does not affect anything else in his paper.

where $\{\theta_i^v, \phi_i^v\}_{i=1}^{12}$ are coordinates of the vertices of an icosahedron inscribed in the unit sphere, w_v their associated weight, N_g is the number of generators with coordinates $\left\{\theta^{(j)}, \phi^{(j)}\right\}_{j=1}^{N_g}$ and weights $\{w_j\}_{j=1}^{N_g}$. For each $g_i \in G$, we denote $\left(\theta_i^{(j)}, \phi_i^{(j)}\right) = \left(g_i^{-1}\theta^{(j)}, g_i^{-1}\phi^{(j)}\right)$. For this quadrature rule, we fix the positions of vertices and, hence, do not consider them as unknowns. The subscript v indicates that the vertices are held fixed. Therefore, for this type of quadrature there are $3N_g+1$ unknown generator coordinates and weights, although there are the total of $60N_g + 12$ nodes.

The second type of quadrature has nodes at the fixed vertices of an icosahedron and one generator with a fixed position at the projection of the center of an icosahedron face onto the sphere which gives rise to 20 points on the sphere. We assume that all other generators give rise to orbits of length 60. Thus, we have

(3.2)
$$Q_{vf}(f) = w_v \sum_{i=1}^{12} f(\theta_i^v, \phi_i^v) + w_f \sum_{i=1}^{20} f\left(\theta_i^f, \phi_i^f\right) + \sum_{j=1}^{N_g} w_j \sum_{i=1}^{60} f\left(\theta_i^{(j)}, \phi_i^{(j)}\right),$$

where $\left\{\theta_i^f, \phi_i^f\right\}_{i=1}^{20}$ are coordinates of the face centers of the icosahedron projected onto the sphere and w_f is the associated weight. For this quadrature there are $3N_g + 2$ unknown generator coordinates and weights, with a total of $60N_g + 32$ nodes.

The third type of quadrature has nodes at the fixed vertices of an icosahedron and one generator with a fixed position at the projection onto the sphere of the mid-point of an edge giving rise to 30 fixed nodes of the quadrature. We have

(3.3)
$$Q_{ve}(f) = w_v \sum_{i=1}^{12} f(\theta_i^v, \phi_i^v) + w_e \sum_{i=1}^{30} f(\theta_i^e, \phi_i^e) + \sum_{j=1}^{N_g} w_j \sum_{i=1}^{60} f\left(\theta_i^{(j)}, \phi_i^{(j)}\right),$$

where $\{\theta_i^e, \phi_i^e\}_{i=1}^{30}$ are coordinates of the projection onto the sphere of the mid-points of edges of the icosahedron and w_e is the associated weight. For this quadrature there are $3N_g + 2$ unknown generator coordinates and weights, with a total of $60N_g + 42$ nodes.

Finally, the fourth type of quadrature has as fixed nodes vertices and projections of both face centers and edge midpoints of the icosahedron. We have

(3.4)
$$\begin{aligned} Q_{vfe}(f) &= w_v \sum_{i=1}^{12} f(\theta_i^v, \phi_i^v) + w_f \sum_{i=1}^{20} f\left(\theta_i^f, \phi_i^f\right) \\ &+ w_e \sum_{i=1}^{30} f(\theta_i^e, \phi_i^e) + \sum_{j=1}^{N_g} w_j \sum_{i=1}^{60} f\left(\theta_i^{(j)}, \phi_i^{(j)}\right). \end{aligned}$$

For this quadrature we have $3N_g + 3$ unknown generator coordinates and weights, with the total of $60N_g + 62$ nodes.

Using Theorem 2.2 or 2.3, we determine the number of invariant functions in the subspace $\mathcal{H}_n$. Theorem 2.1 allows us to limit the number of equations to not exceed the number of invariant functions. Ideally, when constructing a system of equations for the generator coordinates and weights, we would like to match the number of equations to the number of unknowns. For example, to construct a quadrature that integrates exactly the subspace $\mathcal{P}_{23}$, we must integrate the 10 invariant functions in $\mathcal{P}_{23}$. Therefore, we have 10 equations and, using quadrature (3.1), we have $3N_g + 1$ unknowns, where N_g is the number of generators. Setting $3N_g + 1 = 10$ gives $N_g = 3$ and, thus, we look for a quadrature with $192 = 3 \times 60 + 12$ nodes. We solve the corresponding system (see Section 3.2) and obtain a solution, thus verifying its existence directly. We illustrate a set of 7212 nodes that exactly integrates $\mathcal{P}_{145}$ in Figure 3.2. This set of nodes was found using the quadrature Q_v in (3.1).

However, it appears that in some cases so constructed system of equations may not have a solution. Our conclusion is based on the behavior of Newton's iteration and, so far, has not been verified analytically. In such cases, we reduce the number of equations by removing those from the subspace of the highest degree and solve a formally under determined system. We note that in this situation Newton's iteration may not converge quadratically and the resulting quadratures may be less efficient than the count of invariants suggests. However, the reduction in efficiency is negligible for practical purposes. We also note that there may be more than one solution of these equations with different positive weights. In all cases, we directly verify the resulting quadratures for all spherical harmonics.

It is also possible to set two or more of the generator weights equal, thereby reducing the number of unknowns. We have confirmed numerically the existence of quadratures where some of the generator weights are identical. We note that there has been interest in constructing quadratures for the sphere where all weights are equal, i.e., so-called spherical t-designs (see, e.g., [6] and references therein). The approach outlined above allows us to address this problem as well. We note, however, that it might be more natural to pose a problem of finding quadratures with two or more distinct weights depending on the type of quadrature in (3.1-3.4), where we set $w_j = w_1$ for all $j = 2, \ldots, N_g$.

Remark. For quadratures Q_{ve} and Q_{vfe}, the number of unknowns may be slightly different if the node is on an edge but not at its center. In this case, the orbit has length 60 as in the general case, but there are only 2 degrees of freedom since the node is constrained to lie on the great circle joining two vertices of the icosahedron.

We also note that additional quadratures may be constructed by using the full icosahedral group that includes reflections. In this paper, we focus

only on quadratures (3.1-3.4) and will report results of developing other quadratures in a future paper.

3.1. **Efficiency of quadratures on the sphere.** A useful way of measuring the efficiency of a quadrature was suggested in [31] using the ratio of the dimension of the subspace to be integrated to the (maximum) number of degrees of freedom in the quadrature rule (two coordinates and a weight for each node):

$$\eta = \frac{(N+1)^2}{3M}, \tag{3.5}$$

where M is the number of nodes. If $\eta = 1$, we call the quadrature optimal. Remarkably, there are a few special cases where η is slightly greater than 1, see [31]. However, in general the efficiency is less than 1. As the number of nodes M increases, the efficiency of each of the four types of quadratures, Q_v, Q_{vf}, Q_{ve} and Q_{vfe}, improves and approaches 1. In Figure 3.1 we display the potential efficiency of quadrature Q_v as a function of the degree N of subspace $\mathcal{P}_N$ using Theorem 2.2 or 2.3 to count invariants and superimpose the actual efficiencies of computed quadratures. The behavior of efficiency of other quadratures in (3.2-3.4) is similar.

For comparison, the efficiency of the standard discretization of the sphere, using equally spaced nodes in the azimuthal direction and Gauss-Legendre nodes in polar direction, is $\eta_{\text{st}} = 2/3$. Specifically, for a maximum order and degree N, we need at least $N+1$ equally spaced nodes to integrate in the azimuthal direction over the interval $[0, 2\pi)$ and $(N+1)/2$ nodes to integrate in the polar direction with a Gauss-Legendre quadrature over the interval $[0, \pi]$, so that $M = (N+1)^2/2$. The efficiency of the standard quadrature is also illustrated in Figure 3.1.

Although it is beneficial to have a highly efficient quadrature, it is the near uniform distribution of nodes that is the key property of quadratures with icosahedral symmetry. As mentioned in the introduction, clustering of nodes is detrimental for many applications. For example, the smallest distance between nodes determines the maximum time step size when solving PDEs on the sphere. Hence, when using the standard discretization of the sphere, dynamics near the poles forces unnecessarily small time steps to be taken. Although there are procedures to deal with this problem (see e.g. [21]), with our new quadratures the maximum time step size is determined by the dynamics rather than the grid.

3.2. **Iterative method for computing quadratures via Newton's iteration.** We are now in a position to describe our algorithm for finding nodes and weights for quadratures invariant under the icosahedral group. Since the algorithm is the same for all quadratures (3.1–3.4), we use the generic notation Q to denote any one of the four types. For a given N, we first use Theorem 2.2 or 2.3 to determine those n, $0 \le n \le N$, for which $S(n) \neq 0$. This gives a set of values of n which we denote as $\mathcal{N}_N$. For example, we

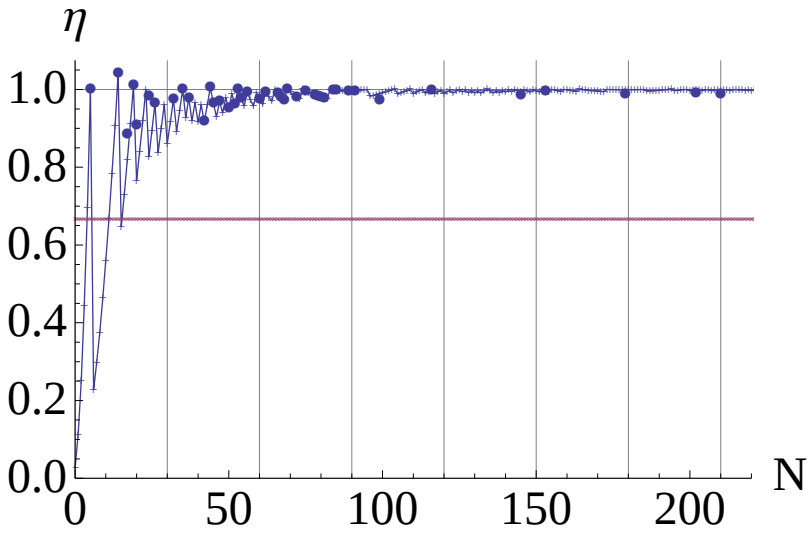

FIGURE 3.1. Potential efficiency (3.5) of quadrature (3.1) as a function of degree N of subspace $\mathcal{P}_N$ computed using Theorems 2.2 or 2.3. Fast oscillations of η for small N are due to the sensitivity of the number of nodes to arithmetic requirements of icosahedral invariance. Note that in a few cases the efficiency is slightly greater than 1. Vertical lines are at locations $|G|\, j/2,\ j = 0, 1, \ldots$, where $|G| = 60$ is the order of icosahedral rotation group. For comparison, efficiency of the standard quadrature $\eta_{\mathrm{st}} = 2/3$ is also shown. Solid dots indicate the efficiency of computed quadratures using our approach.

obtain $\mathcal{N}_{21} = \{0, 6, 10, 12, 15, 16, 18, 20, 21\}$. We now define the set of orders m associated with a fixed degree n as

$$\mathcal{M}_n = \begin{cases} m = 2\,(l-1)\,,\ l = 1, 2, \ldots S\,(n) & \text{if } n \text{ is even} \\ m = 2l,\ l = 1, 2, \ldots S\,(n) & \text{if } n \text{ is odd} \end{cases}. \tag{3.6}$$

Note that for odd m, $Q\,(Y_n^m)$ vanishes identically by symmetry. Using indices $\mathcal{M}_n$ with $n \in \mathcal{N}_N$, we now construct the equations

$$F_{n,m} \equiv Q\,(Y_n^m) - I_{n,m} = 0,\ m \in \mathcal{M}_n,\ n \in \mathcal{N}_N, \tag{3.7}$$

where $I_{n,m} = \int_{\mathbb{S}^2} Y_n^m d\Omega = \sqrt{4\pi}\delta_{n,0}\delta_{m,0}$ and δ is the Kronecker delta. The collection of equations in (3.7) is a system of nonlinear equations for the generator coordinates and weights and the weights associated with the fixed nodes. The group actions in $Q\,(Y_n^m)$ (see (3.1–3.4)) are carried out using quaternionic multiplication, as described in Section 2.2. Our formulation implicitly assumes that the invariants functions generated numerically from (3.6) for $n \in \mathcal{N}_N$ are independent. It has been our observation that this is

the case since any missing invariant functions would have been discovered during *a posteriori* verification of quadratures.

Recall that Newton's method for solving the system of nonlinear equations $\mathbf{F}(\mathbf{x}) = \mathbf{0}$ with $\mathbf{F} : \mathbb{R}^{n'} \to \mathbb{R}^n$, where $n' \leq n$, is the iteration

$$\mathbf{x}_{i+1} = \mathbf{x}_i - \mathbf{J}_i^{\dagger}\mathbf{F}_i, \tag{3.8}$$

starting with some initial vector $\mathbf{x}_0$, where $\mathbf{J}$ is the Jacobian of $\mathbf{F}$,

$$\mathbf{J}_{ij} = \frac{\partial F_i}{\partial x_j}, \tag{3.9}$$

and $\mathbf{J}_i^{\dagger}$ is its generalize inverse.

Writing (3.7) in vector notation $\mathbf{F} = \mathbf{0}$, we use (3.8) to solve for the generator coordinates and weights and the weight associated with the fixed nodes. The Jacobian is calculated analytically, as described in Appendix. As a way of finding initial weights, we use the initial node distribution to form and solve the linear system

$$\mathcal{K}\mathbf{w} = 4\pi \mathrm{I},$$

where the matrix $\mathcal{K}$ has entries $\mathcal{K}_{ij} = K(\boldsymbol{\omega}_i \cdot \boldsymbol{\omega}_j)$, vector $\mathrm{I} = (1, 1, \ldots, 1)^t$, $\mathrm{I} \in \mathbb{R}^M$, and $\mathbf{w}$ is the vector of initial weights. Construction of the initial node distribution is described in Section 3.3 below.

In Figure 3.2 we illustrate a quadrature with 7212 nodes that integrates functions in $\mathcal{P}_{145}$. The lighter colored nodes correspond to the vertices of the icosahedron, while the darker colored nodes are those constructed by group action on the generators. Note that each of the darker colored nodes has 6 nearest neighbors, whereas the vertices of the icosahedron have only 5 nearest neighbors. So far the largest subspace we have constructed quadratures for is $\mathcal{P}_{210}$.

3.3. **Generation of initial grid.** At first, as the initial node distribution, we used spherical codes with icosahedral symmetry generated by Hardin, Sloane and Smith [16]. In using such initial distributions, we observed that the key to convergence of Newton's method has been the structural similarity of the initial grid with the final quadrature grid. This led us to a simple construction that assures such structural similarity.

Let us start by generating a lattice in the plane formed by equilateral triangles,

$$\{m\mathbf{e}_1 + n\mathbf{e}_2\}_{m,n\in\mathbb{Z}},$$

with the lattice vectors $\mathbf{e}_1 = (1, 0)$ and $\mathbf{e}_2 = (1/2, \sqrt{3}/2)$. We then select three points,

$$P_0 = (0, 0), \quad P_1 = t\mathbf{e}_1 + s\mathbf{e}_2, \quad P_2 = -s\mathbf{e}_1 + (t + s)\mathbf{e}_2,$$

on the lattice to form an equilateral triangle with vertices P_0, P_1 and P_2, where $t, s \in \mathbb{N}$ are positive integers. Indeed, it is easy to check that $|P_0P_1|^2 = |P_0P_2|^2 = |P_1P_2|^2 = s^2 + ts + t^2$. We consider t and s as parameters which

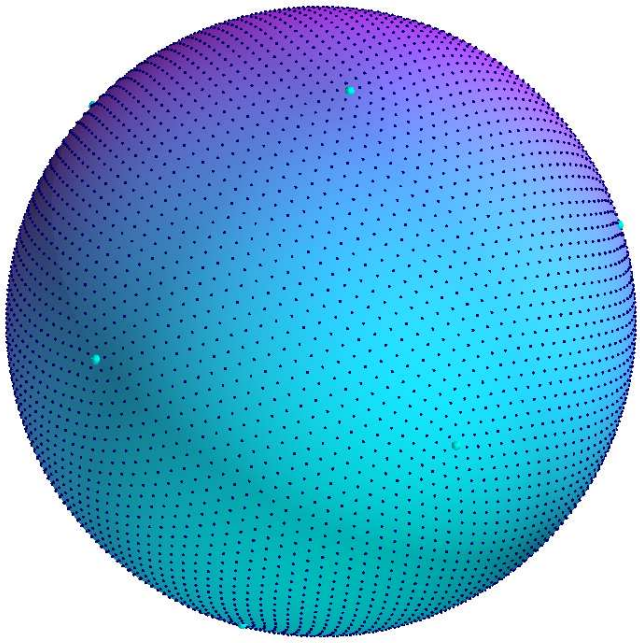

FIGURE 3.2. Positions of 7212 quadrature nodes of a quadrature integrating exactly all spherical harmonics in the subspace of maximal order and degree 145. This quadrature has efficiency $\eta = 0.98521....$

uniquely determine the number and type of generators for which the triangle $P_0P_1P_2$ serves as a template. Thus, t and s uniquely determine the total number of unknown parameters in the nonlinear system (3.7). We illustrate this construction in Figure 3.3.

The center of the triangle $P_0P_1P_2$ is at the point

$$P_c = (t-s)/3\,\mathbf{e}_1 + (t+2s)/3\,\mathbf{e}_2 = \left(t/2, (t+2s)/(2\sqrt{3})\right),$$

which may or may not be a point of the lattice. If the center coincides with a lattice point, then the type of quadrature is one with a face-centered node. In the same manner, for some choices of parameters t and s, there might be points on the sides of the triangle and, in such case, it leads to a quadrature with edge-centered nodes. As we pointed out already, the type of quadrature affects the count of independent variables.

In order to find the generators, we select nodes in the interior of a fundamental region of the icosahedral rotation group, defined by connecting the center of the triangle with any two of its vertices [14]. We use the triangle $P_0P_1P_c$. See Figure 3.3 for an illustration of this particular fundamental region. We note that by definition, acting with the icosahedral rotation group

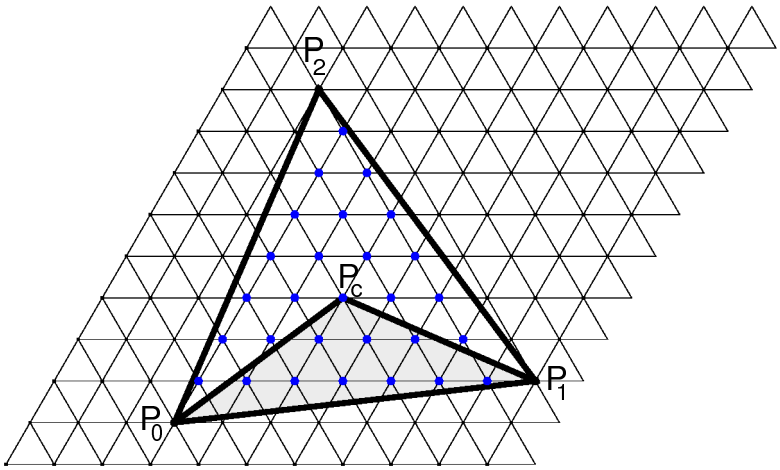

FIGURE 3.3. A grid template on a face of the icosahedron. Here there are 9 generators with orbits of length 60 and 1 node at the face center with orbit length 20, yielding 28 nodes in the interior of the triangle and 572 total nodes on the sphere. The resulting quadrature found using Newton's method integrates the subspace of maximum order and degree $N = 40$. One of the possible 3 fundamental region is shown shaded.

on points inside the fundamental region will produce points on all faces of the icosahedron and, thus, it is sufficient to consider only points inside that region and, in addition, points on the sides of the triangle $P_0P_1P_c$.

In placing points from the fundamental region to the surface of the icosahedron inscribed into the unit sphere, it is convenient to use the barycentric system of coordinates associated with the triangle $P_0P_1P_c$. The barycentric coordinates (τ_0, τ_1, τ_c) of a lattice point $\{m\mathbf{e}_1 + n\mathbf{e}_2\}$ are found by explicitly solving the 3×3 linear system

$$\begin{aligned} \tau_0 + \tau_1 + \tau_c &= 1, \\ \tau_1(2t + s) + \tau_c t &= 2m + n, \\ \tau_1 s + \tau_c(t + s) &= n, \end{aligned}$$

which yields

$$\begin{aligned} \tau_0 &= \frac{s^2 + (s - t)\, m + st + t^2 - (s + 2t)\, n}{s^2 + st + t^2}, \\ \tau_1 &= \frac{(2m + n)\, s + (m - n)\, t}{s^2 + st + t^2}, \\ \tau_c &= \frac{3\,(nt - ms)}{s^2 + st + t^2}. \end{aligned}$$

We recall that a point is inside the triangle $P_0P_1P_c$ if $\tau_0, \tau_1, \tau_c > 0$ and it is on a side if one of the barycentric coordinates is equal to 0. In order

to position the generators onto the sphere, we first map the points from the fundamental region formed by the triangle $P_0P_1P_c$ to a face of the icosahedron. Let vectors $\tilde{P}_0, \tilde{P}_1, \tilde{P}_2 \in \mathbb{R}^3$, define a face of the icosahedron and $\tilde{P}_c \in \mathbb{R}^3$ the center of the face. A point with the barycentric coordinates (τ_0, τ_1, τ_c) with respect to the triangle $P_0P_1P_c$ is then mapped to the point $\tau_0\tilde{P}_0+\tau_1\tilde{P}_1+\tau_c\tilde{P}_c$. We then project this point radially outward to the surface of the unit sphere. Using the resulting generators, we apply group actions to produce all the nodes on the surface of sphere.

Finally we note that as the number of generators grows, we use previously constructed quadrature nodes to map a grid template on a face of the icosahedron to the sphere. We use the barycentric coordinates of points within the corresponding triangles on a face of the icosahedron formed by preimages of previous quadratures nodes on the sphere.

4. An analogue of Lagrange interpolation and an alternative representation for rotationally invariant subspaces of $L^2\left(\mathbb{S}^2\right)$

Using the results in Sections 2 and 3, we now construct an alternative representation for functions on invariant subspaces of $L^2\left(\mathbb{S}^2\right)$. Let us discretize (2.7) and (2.8) using quadratures developed in Section 3. The quadrature must be chosen so that it integrates exactly subspaces of order and degree at least $2N$, since this is the maximal order and degree of the product $K\left(\boldsymbol{\omega}\cdot\boldsymbol{\omega}'\right) f\left(\boldsymbol{\omega}'\right)$ in (2.7). Using such a quadrature, we have the identity,

$$f\left(\boldsymbol{\omega}\right) = \sum_{j=1}^{M} K\left(\boldsymbol{\omega}\cdot\boldsymbol{\omega}_j\right) w_j f\left(\boldsymbol{\omega}_j\right), \tag{4.1}$$

where $\boldsymbol{\omega}_j = (\cos\phi_j \sin\theta_j, \sin\phi_j \sin\theta_j, \cos\theta_j)$ are unit vectors denoting the coordinates of the quadrature nodes and w_j the associated weights.

We observe that if $f \in \mathcal{P}_N$, then (4.1) provides an exact reconstruction of the function f from its values $f\left(\boldsymbol{\omega}_1\right), f\left(\boldsymbol{\omega}_2\right), \ldots, f\left(\boldsymbol{\omega}_M\right)$. Comparing (4.1) with standard Lagrange interpolation, we see that the functions $\left\{K\left(\boldsymbol{\omega}\cdot\boldsymbol{\omega}_j\right) w_j\right\}_{j=1}^{M}$ play a role similar to that of Lagrange interpolating polynomials and, therefore, we may think of (4.1) as an analogue of Lagrange interpolation on the sphere. Formulas of this type have appeared in [36, 37] using the standard quadratures for the sphere that are not invariant under the action of a discrete rotation group. Due to concentration of nodes near the poles and lack of invariance, the properties of representations obtained in these papers differ from that in (4.1).

Since every function $f \in \mathcal{P}_N$ may be written as a linear combination of functions $\left\{K\left(\boldsymbol{\omega}\cdot\boldsymbol{\omega}_j\right) w_j\right\}_{j=1}^{M}$, we may use such linear combinations to represent all functions in $\mathcal{P}_N$. We avoid calling $\left\{K\left(\boldsymbol{\omega}\cdot\boldsymbol{\omega}_j\right) w_j\right\}_{j=1}^{M}$ a basis since the number of these functions exceeds the dimension of the subspace $\mathcal{P}_N$; however, effectively they play the same role as a basis for $\mathcal{P}_N$. We elaborate

on this further below and note that an attempt to use the same number of functions $K(\boldsymbol{\omega}\cdot\boldsymbol{\omega}_j)$ as the dimension of $\mathcal{P}_N$ leads to ill-conditioned systems [38, 10].

Let us now consider $f\in\mathcal{P}_N$ and evaluate (4.1) at the quadrature nodes $\{\boldsymbol{\omega}_i\}_{i=1}^M$. We obtain

$$\sqrt{w_i}f(\boldsymbol{\omega}_i)=\sum_{j=1}^{M}\left(\sqrt{w_i}\,K(\boldsymbol{\omega}_i\cdot\boldsymbol{\omega}_j)\sqrt{w_j}\right)\left(\sqrt{w_j}f(\boldsymbol{\omega}_j)\right),$$

where we multiplied both sides by $\sqrt{w_i}$. Denoting $\tilde{f}_i=\sqrt{w_i}f(\boldsymbol{\omega}_i)$ and $K_{ij}=\sqrt{w_i}\,K(\boldsymbol{\omega}_i\cdot\boldsymbol{\omega}_j)\sqrt{w_j}$, we obtain the matrix identity

$$\tilde{f}_i=\sum_{j=1}^{M}K_{ij}\tilde{f}_j, \tag{4.2}$$

where the matrix $\mathcal{K}$ with entries K_{ij} is a projector with eigenvalues either 1 or 0. Since the number of nodes M for the projector on a subspace of dimension $(N+1)^2$ is at least $(2N+1)^2/3$, it asymptotically exceeds the dimension of the subspace $\mathcal{P}_N$ by a factor $\approx 4/3$. This results in zero eigenvalues to match the dimension of $\mathcal{P}_N$ and the range of $\mathcal{K}$. For example, the dimension of $\mathcal{P}_7$ is 64 and we need a quadrature with the minimum of $M=72$ nodes so that $\mathcal{K}$ has 64 eigenvalues equal to 1 and 8 eigenvalues equal to 0. We note that given the projector, the null space does not cause problems in numerical computations since it allows us to work on the range coinciding with $\mathcal{P}_N$. The near optimal number of nodes does reduce the number of unknowns in the problem of scattered data interpolation on the sphere, a problem we plan to consider elsewhere.

In Figure 4.1 we show a cross section of $K(\boldsymbol{\omega}\cdot\mathbf{e}_z)$ through the z axis, with the maximum value of K normalized to 1.

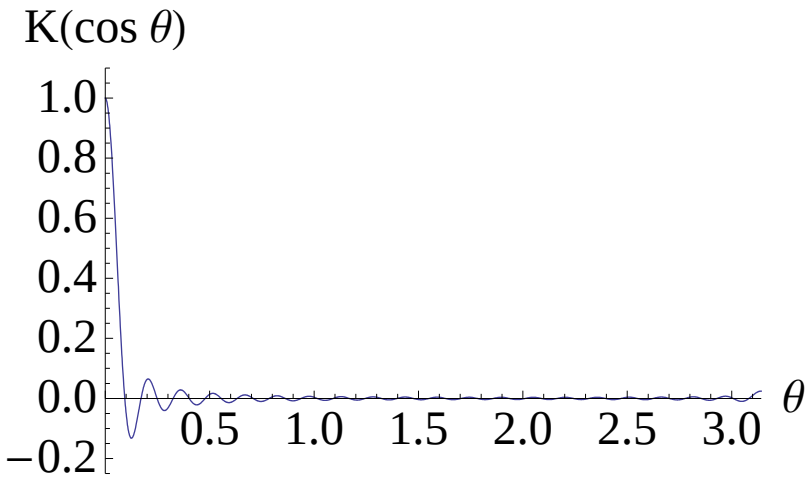

FIGURE 4.1. Cross-section of normalized kernel with $N=40$.

5. Algorithms associated with icosahedral grids

For efficient use of the quadratures developed in this paper, we need fast algorithms for evaluation of sums on these grids. Currently we only have $\mathcal{O}(N^3)$ algorithms for this purpose and are working on the development of faster $\mathcal{O}(N^2 \log N)$ methods. We note that although there are $\mathcal{O}(N^2 \log N)$ algorithms for evaluation of spherical harmonics, for most of them the break-even point in comparison with the usual $\mathcal{O}(N^3)$ versions is quite high [41]. Here we describe $\mathcal{O}(N^3)$ algorithms for the numerical implementation of the representation (4.1). We consider two approaches: the first is based on the ideas in [21] and the second on the Unequally Spaced Fast Fourier Transform (USFFT) [9, 3, 28].

5.1. Application of kernel K using the Christoffel-Darboux formula.

The key observation in [21] is that the numerical evaluation of (4.1) may be accelerated by using the addition theorem and the Christoffel-Darboux formula, provided that it is implemented via a fast algorithm. The kernel K may be written as

$$\begin{aligned} K(\boldsymbol{\omega}\cdot\boldsymbol{\omega}') &= \frac{1}{2\pi}\sum_{m=-N}^{N}\left(\frac{(N+1)^2-m^2}{4(N+1)^2-1}\right)^{1/2} \\ &\quad \left[\frac{\overline{P}_{N+1}^m(\cos\theta)\overline{P}_N^m(\cos\theta')-\overline{P}_N^m(\cos\theta)\overline{P}_{N+1}^m(\cos\theta')}{\cos\theta-\cos\theta'}\right] e^{im(\phi-\phi')}, \end{aligned} \tag{5.1}$$

with $\overline{P}_N^m$ the normalized associated Legendre functions (see Section 2) and $\boldsymbol{\omega}\cdot\boldsymbol{\omega}' = \cos\theta\cos\theta' + \sin\theta\sin\theta'\cos(\phi-\phi')$. With an appropriate rotation of coordinates, the quadrature nodes can be seen to lie on planes of constant polar angle, with five points equally spaced in azimuthal angle on each plane. We write the coordinates of the quadrature nodes in plane i as $\left(\theta_i, \frac{2\pi}{5}k+\delta_i\right)$, $k=0,1,2,3,4$, where δ_i is the relative shift in azimuth from plane $i-1$ to plane i. We label the planes such that $\theta_{i-1}<\theta_i$ and set $\delta_1=0$. Substituting (5.1) into (4.1), we need to evaluate the sum

$$\begin{aligned} f(\theta,\phi) &= \frac{1}{2\pi}\sum_{m=-N}^{N}\left(\frac{(N+1)^2-m^2}{4(N+1)^2-1}\right)^{1/2}\sum_{i=1}^{N_{\text{planes}}} w_i \\ &\quad \left[\frac{\overline{P}_{N+1}^m(\cos\theta)\overline{P}_N^m(\cos\theta_i)-\overline{P}_N^m(\cos\theta)\overline{P}_{N+1}^m(\cos\theta_i)}{\cos\theta-\cos\theta_i}\right] \\ &\quad e^{im(\phi-\delta_i)}\sum_{k=0}^{4} e^{-i\frac{2\pi mk}{5}} f\left(\theta_i, \frac{2\pi}{5}k+\delta_i\right), \end{aligned} \tag{5.2}$$

where N_{planes} is the number of planes. Following the key idea in [21], we evaluate the summation over the index i in (5.2) using a fast algorithm (e.g., Fast Multipole Method (FMM) as in [21]). However, the quadrature used

in [21] is the standard quadrature with $\mathcal{O}(N)$ Gauss-Legendre nodes in the polar direction (and thus $N_{\text{planes}} \sim N$) and $\mathcal{O}(N)$ equally spaced nodes in the azimuthal direction. Using the Fast Fourier transform to evaluate along the azimuthal direction and FMM to evaluate in the polar direction yields the overall complexity of $\mathcal{O}\left(N^2 \log N\right)$. Unfortunately, in our case the number of planes $N_{\text{planes}} \sim N^2$ thus yielding only an $\mathcal{O}\left(N^3\right)$ algorithm.

5.2. **Application of kernel K using the USFFT.** Since the kernel K may be written as in (2.8), it also has a finite Fourier series representation

$$K\left(\boldsymbol{\omega} \cdot \boldsymbol{\omega}'\right) = \sum_{|n| \leq N} c_n e^{i\, n\, \boldsymbol{\omega} \cdot \boldsymbol{\omega}'}.$$

Substituting this sum into (4.1), changing the order of summations and evaluating at $J \sim \mathcal{O}\left(N^2\right)$ arbitrary points on the sphere, $\{\boldsymbol{\omega}\}_{j=1}^{J}$, yields

$$f\left(\boldsymbol{\omega}_j\right) = \sum_{|n| \leq N} c_n \sum_{i=1}^{M} w_i f\left(\boldsymbol{\omega}_i\right) e^{i\, n\, \boldsymbol{\omega}_j \cdot \boldsymbol{\omega}_i}, \tag{5.3}$$

where M is the total number of quadrature nodes. Recall that $M \sim \mathcal{O}\left(N^2\right)$. The sum in (5.3) may be evaluated in $\mathcal{O}\left(N^3\right)$ operations using USFFT. We split (5.3) as

$$f\left(\boldsymbol{\omega}_j\right) = \sum_{|n| \leq N} c_n g(n\, \boldsymbol{\omega}_j), \tag{5.4}$$

with

$$g\left(n\, \boldsymbol{\omega}_j\right) = \sum_{i=1}^{M} w_i f\left(\boldsymbol{\omega}_i\right) e^{i\, n\, \boldsymbol{\omega}_j \cdot \boldsymbol{\omega}_i}. \tag{5.5}$$

We may view (5.5) as evaluation of function g at $\mathcal{O}\left(N^3\right)$ points $n\, \boldsymbol{\omega}_j$, $|n| \leq N$ and $j = 1, \ldots, J$ (which may be interpreted as frequencies for the purposes of USFFT). Since $|\boldsymbol{\omega}_i| = 1$ in (5.5), fast evaluation of such sums is precisely the task for USFFT. Once we obtain values $g\left(n\, \boldsymbol{\omega}_j\right)$, we compute the sum in (5.4) directly at cost of $\mathcal{O}\left(N^3\right)$.

6. Local and multiresolution representations on the sphere

We expect that grids invariant under the icosahedral group (or other finite rotation groups) will play an important role in constructing efficient and practical local and multiresolution representations of functions on the sphere. In this paper we only point out that the rate of decay and the oscillations of the functions $K(\boldsymbol{\omega} \cdot \boldsymbol{\omega}_i)$ may be altered by extending and bringing gradually to zero the spectrum of the kernel as a projector. We consider these results as preliminary since there might be representations with better localization.

If we were to measure the decay of a function on the sphere using variance defined as

$$\mathrm{Var}\left(f\right) \equiv \frac{\int_{\mathbb{S}^2} \left\|\boldsymbol{\xi} - \langle\boldsymbol{\xi}\rangle\right\|^2 f\left(\boldsymbol{\xi}\right)^2 d\Omega}{\int_{\mathbb{S}^2} f\left(\boldsymbol{\xi}\right)^2 d\Omega}, \tag{6.1}$$

where the mean is defined as

$$\langle\boldsymbol{\xi}\rangle \equiv \frac{\int_{\mathbb{S}^2} \boldsymbol{\xi}\, f\left(\boldsymbol{\xi}\right)^2 d\Omega}{\int_{\mathbb{S}^2} f\left(\boldsymbol{\xi}\right)^2 d\Omega}, \tag{6.2}$$

then we can show that for large N the variance of the kernel K decays only as $\mathcal{O}\left(1/N\right)$.

To improve localization of the kernel, let us consider

$$\tilde{K}\left(\boldsymbol{\omega}\cdot\boldsymbol{\omega}'\right) = K\left(\boldsymbol{\omega}\cdot\boldsymbol{\omega}'\right) + \sum_{n=N+1}^{pN} \frac{2n+1}{4\pi} a_n P_n\left(\boldsymbol{\omega}\cdot\boldsymbol{\omega}'\right), \tag{6.3}$$

where p is the over-sampling factor and the coefficients a_n are chosen to improve localization. Substituting (6.3) into (6.1) and minimizing the result with respect to a_n, we find that the resulting coefficients a_n decrease linearly with a particular (optimal) slope. Using these optimal coefficients, we achieve $\mathrm{Var}\left(\tilde{K}\right) \sim \mathcal{O}\left(1/\left(pN\right)^2\right)$. Since the total number of nodes is also proportional to N^2, this indicates that for a given node the number of neighbors needed to be taken into account to achieve a given accuracy remains constant as N becomes large.

We now show that $\tilde{K}$ may be used as a projector onto $\mathcal{P}_N$. For fixed $\boldsymbol{\omega}$, we have $\tilde{K} \in \mathcal{P}_{pN}$, while $\tilde{K} - K \notin \mathcal{P}_N$. Thus, we obtain

$$K\left(\boldsymbol{\omega}\cdot\boldsymbol{\omega}'\right) = \int_{\mathbb{S}^2} \tilde{K}\left(\boldsymbol{\omega}\cdot\boldsymbol{\nu}\right) K\left(\boldsymbol{\nu}\cdot\boldsymbol{\omega}'\right) d\boldsymbol{\nu}.$$

Now for $f \in \mathcal{P}_N$, we write

$$f\left(\boldsymbol{\omega}\right) = \int_{\mathbb{S}^2} K\left(\boldsymbol{\omega}\cdot\boldsymbol{\omega}'\right) f\left(\boldsymbol{\omega}'\right) d\boldsymbol{\omega}'$$

resulting in

$$\begin{aligned}
\int_{\mathbb{S}^2} \tilde{K}\left(\boldsymbol{\omega}\cdot\boldsymbol{\nu}\right) f\left(\boldsymbol{\nu}\right) d\boldsymbol{\nu} &= \int_{\mathbb{S}^2}\int_{\mathbb{S}^2} \tilde{K}\left(\boldsymbol{\omega}\cdot\boldsymbol{\nu}\right) K\left(\boldsymbol{\nu}\cdot\boldsymbol{\omega}'\right) f\left(\boldsymbol{\omega}'\right) d\boldsymbol{\omega}' d\boldsymbol{\nu} \\
&= \int_{\mathbb{S}^2} K\left(\boldsymbol{\omega}\cdot\boldsymbol{\omega}'\right) f\left(\boldsymbol{\omega}'\right) d\boldsymbol{\omega}' \\
&= f\left(\boldsymbol{\omega}\right),
\end{aligned}$$

so that $\tilde{K}$ is a projector onto $\mathcal{P}_N$. One of the benefits of using $\tilde{K}$ over K is that we may consider fast algorithms exploiting the local nature of $\tilde{K}$. We leave it as a subject for future research.

7. Conclusions

We introduce a general numerical method for constructing quadratures invariant under the icosahedral group which integrate rotationally invariant subspaces of $L^2\left(\mathbb{S}^2\right)$. We note that while the specific results presented here are for the icosahedral rotation group, quadratures invariant under other symmetry groups may be constructed following the same approach. Using these quadratures, we develop an exact representation of functions on rotationally invariant subspaces of $L^2\left(\mathbb{S}^2\right)$, similar to Lagrange interpolation. We describe two algorithms of $\mathcal{O}\left(N^3\right)$ complexity for the numerical use of this representation. Furthermore, we develop a representation with localized functions and describe its properties.

In many ways the results of this paper are just the first step in a program to develop practical methods in a variety of applications that have to deal with the sphere. Further research should involve:

(1) Fast algorithms using these grids that have $\mathcal{O}\left(N^2 \log N\right)$ complexity, hopefully with a low break-even point in comparison with $\mathcal{O}\left(N^3\right)$ algorithms.
(2) A greater variety of localized representations with associated fast algorithms.
(3) Multiresolution representations that maintain a relation with the rotationally invariant subspaces.
(4) Appropriate representations of integral and differential operators on the sphere and their embedding into a variety of applications.

References

[1] J.P. Antoine, L. Demanet, L. Jacques, and P. Vandergheynst. Wavelets on the sphere: implementation and approximations. *Appl. Comput. Harmon. Anal.*, 13(3):177–200, 2002.
[2] G. Backus, R. Parker, and C. Constable. *Foundations of Geomagnetism*. Cambridge University Press, 1996.
[3] G. Beylkin. On the fast Fourier transform of functions with singularities. *Appl. Comput. Harmon. Anal.*, 2(4):363–381, 1995.
[4] G. Beylkin and R. Cramer. Toward multiresolution estimation and efficient representation of gravitational fields. *Celestial Mechanics and Dynamical Astronomy*, 84(1):87–104, 2002.
[5] D. Colton and R. Kress. *Inverse Acoustic and Electromagnetic Scattering Theory*. Springer-Verlag, 1992.
[6] J.H. Conway and N.J.A. Sloane. *Sphere Packings, Lattices and Groups*. Springer, third edition, 1999.
[7] R. Cools. Constructing cubature formulae: the science behind the art. *Acta Numerica*, 6:1–54, 1997.
[8] I. Daubechies, I. Guskov, P. Schröder, and W. Sweldens. Wavelets on irregular point sets. *R. Soc. Lond. Philos. Trans. Ser. A Math. Phys. Eng. Sci.*, 357(1760):2397–2413, 1999.
[9] A. Dutt and V. Rokhlin. Fast Fourier transforms for nonequispaced data. *SIAM J. Sci. Comput.*, 14(6):1368–1393, 1993.

[10] N. Fernandez. Localized polynomial bases on the sphere. *Electronic Transactions on Numerical Analysis*, 19:84–93, 2005.
[11] N. Fernandez and J. Prestin. Interpolatory band-limited wavelet bases on the sphere. *Constructive Approximation*, 23(1):79–101, 2005.
[12] W. Freeden, T. Gervens, and M. Schreiner. *Constructive Approximation on the Sphere with Applications to Geomathematics*. Oxford University Press, 1998.
[13] I.S. Gradshteyn and I. M. Ryzhik. *Table of Integrals, Series, and Products*. Academic Press, 5th edition, 1994.
[14] L.C. Grove and C.T. Benson. *Finite Reflection Groups*. Springer-Verlag, 1985.
[15] F. Guilloux, G. Faÿ, and J. Cardoso. Practical wavelet design on the sphere. *Appl. Comput. Harmon. Anal.*, 26(2):143–160, 2009.
[16] R. H. Hardin, N. J. A. Sloane, and W. D. Smith. Tables of spherical codes with icosahedral symmetry. *Published electronically at http://www.research.att.com/ njas/icosahedral.codes/*, 2000.
[17] D. J. Haxton. Lebedev discrete variable representation. *Journal of Physics B: Atomic, Molecular and Optical Physics*, 40:4443–4451, 2007.
[18] W.A. Heiskanen and H. Moritz. *Physical Geodesy*. W.H. Freeman and Company, 1967.
[19] M. Holschneider. Continuous wavelet transforms on the sphere. *J. Math. Phys.*, 37(8):4156–4165, 1996.
[20] M. Holschneider and I. Iglewska-Nowak. Poisson wavelets on the sphere. *J. Fourier Anal. Appl.*, 13(4):405–419, 2007.
[21] R. Jakob-Chien and B. K. Alpert. A fast spherical filter with uniform resolution. *J. Comput. Phys.*, 136:580–584, 1997.
[22] S. I. Konyaev. Quadratures of Gaussian type for the sphere invariant under the icosahedral group with inversion. *Mathematicheskie Zametki*, 25(4):629–634, 1977.
[23] S. I. Konyaev. Formulas for numerical integration on the sphere. In *Imbedding theorems and their applications*, Trudy Sem. S. L. Soboleva, No. 1, pages 75–82. Akad. Nauk SSSR Sibirsk. Otdel. Inst. Mat., Novosibirsk, 1982.
[24] J. B. Kuipers. *Quaternions and rotation sequences: A primer with applications to orbits, aerospace and virtual reality*. Princeton University Press, 1999.
[25] Q. T. Le Gia and H. N. Mhaskar. Localized linear polynomial operators and quadrature formulas on the sphere. *SIAM Journal of Numerical Analysis*, 47(1):440–466, 2008.
[26] V. I. Lebedev. Quadratures on a sphere. *Zh. vychisl. Mat. mat. Fiz.*, 16(2):293–306, 1976.
[27] V.I. Lebedev and D.N. Laikov. A quadrature formula for the sphere of the 131st algebraic order of accuracy. *Doklady Mathematics*, 59(3):477–481, 1999. Translated from Doklady Akademii Nauk, Vol. 36, No. 6, 1999, pp. 741-745.
[28] J-Y. Lee and L. Greengard. The type 3 nonuniform FFT and its applications. *J. Comput. Phys.*, 206(1):1–5, 2005.
[29] C. Lessig. Orthogonal and symmetric Haar wavelets on the sphere. Master's thesis, Department of Computer Science, University of Toronto, 2007.
[30] J. C. Light, I. P. Hamilton, and J. V. Lill. Generalized discrete variable approximation in quantum mechanics. *Journal of Chemical Physics*, 82(3):1400–1409, 1985.
[31] A.D. McLaren. Optimal numerical integration on a sphere. *Mathematics of Computation*, 17(84):361–383, 1963.
[32] B. Meyer. On the symmetries of spherical harmonics. *Canadian J. Math.*, 6:135–157, 1954.
[33] T. Molien. Über die Invarianten der linearen Substitutionsgruppen. *S. B. Akad. Wiss. Berlin*, 2:1152–1156, 1897.
[34] A.S. Popov. Cubature Formulas on a Sphere Invariant under the Icosahedral Rotation Group. *Numerical Analysis and Aplications*, 1(4):355–361, 2008.

[35] P. Schröder and W. Sweldens. Spherical wavelets: efficiently representing functions on the sphere. In *Proceedings of the 22nd annual conference on Computer graphics and interactive techniques*, pages 161–172. SIGGRAPH, ACM, New York, NY, USA, 1995.
[36] I. H. Sloan. Polynomial interpolation and hyperinterpolation over general regions. *Journal of Approximation Theory*, 83:238–254, 1995.
[37] I. H. Sloan and R. S. Womersley. Constructive polynomial approximation on the sphere. *Journal of Approximation Theory*, 103:91–118, 2000.
[38] I. H. Sloan and R. S. Womersley. Good approximation on the sphere, with application to geodesy and the scattering of sound. *J. Comput. Appl. Math.*, 149(1):227–237, 2002. Scientific and engineering computations for the 21st century—methodologies and applications (Shizuoka, 2001).
[39] S. L. Sobolev. Cubature formulas on the sphere invariant under finite groups of rotations. *Doklady Akademii Nauk SSSR*, 146:310–313, 1962.
[40] S.L. Sobolev. *Cubature formulas and modern analysis*. Nauka Publishers, 1974.
[41] W.F. Spotz and P.N. Swarztrauber. A performance comparison of associated Legendre projections. *Journal of Computational Physics*, 168(2):339 – 355, APR 10 2001.
[42] A.H. Stroud. *Approximate Calculation of Multiple Integrals*. Prentice-Hall, 1971.
[43] M. Taylor, J. Tribbia, and M. Iskandarani. The spectral element method for the shallow water equations on the sphere. *J. Comp. Physics*, 130:92–108, 1997.
[44] D. L. Williamson, J. B. Drake, J. J. Hack, R. Jakob, and P. N. Swarztrauber. A standard test set for numerical approximations to the shallow water equations in spherical geometry. *J. Comput. Phys.*, 102:211–224, 1992.

8. Appendix

Evaluation of the Jacobian. Here we give details of computing the Jacobian of the nonlinear system (3.7). Let $(\cos\phi\sin\theta, \sin\phi\sin\theta, \cos\theta)$ be spherical coordinates of a point on the unit sphere which we may also write as a quaternion,

$$\boldsymbol{\nu} = \mathbf{i}\cos\phi\sin\theta + \mathbf{j}\sin\phi\sin\theta + \mathbf{k}\cos\theta.$$

Applying a rotation as quaternion multiplication, $\mathbf{q}_r\boldsymbol{\nu}\mathbf{q}_r^{-1}$, we get quaternion of the form

$$\boldsymbol{\nu}' = \mathbf{i}f(\theta,\phi) + \mathbf{j}g(\theta,\phi) + \mathbf{k}h(\theta,\phi) = \mathbf{i}\cos\phi'\sin\theta' + \mathbf{j}\sin\phi'\sin\theta' + \mathbf{k}\cos\theta',$$

where the functions f, g, and h describe the action of the group element. Hence, the rotated point has spherical coordinates

$$\cos\theta' = h(\theta,\phi), \quad \cos\phi' = \frac{f(\theta,\phi)}{\sqrt{f(\theta,\phi)^2 + g(\theta,\phi)^2}}, \quad \sin\phi' = \frac{g(\theta,\phi)}{\sqrt{f(\theta,\phi)^2 + g(\theta,\phi)^2}}.$$

Thus, the spherical harmonic

$$Y_n^m(\theta,\phi) = C_n^m P_n^m\left(\cos(\theta)\right)\left(\cos\phi + i\sin\phi\right)^m,$$

after rotation is written as

$$Y_n^m(\theta',\phi') = C_n^m P_n^m\left(\cos\theta'\right)\left(\cos\phi' + i\sin\phi'\right)^m, \tag{8.1}$$

where C_n^m is a normalization constant. We now compute the partial derivatives of (8.1) with respect to θ and ϕ. We obtain

$$\begin{aligned}\frac{\partial}{\partial\theta}Y_n^m(\theta',\phi') &= C_n^m\left(P_n^m\right)'\left(\cos\theta'\right)\left(\cos\phi'+i\sin\phi'\right)^m\frac{\partial\cos\theta'}{\partial\theta}\\ &+ mC_n^mP_n^m\left(\cos\theta'\right)\left(\cos\phi'+i\sin\phi'\right)^{m-1}\left(\frac{\partial\cos\phi'}{\partial\theta}+i\frac{\partial\sin\phi'}{\partial\theta}\right)\end{aligned}$$

and

$$\begin{aligned}\frac{\partial}{\partial\phi}Y_n^m(\theta',\phi') &= C_n^m\left(P_n^m\right)'\left(\cos\theta'\right)\left(\cos\phi'+i\sin\phi'\right)^m\frac{\partial\cos\theta'}{\partial\phi}\\ &+ mC_n^mP_n^m\left(\cos\theta'\right)\left(\cos\phi'+i\sin\phi'\right)^{m-1}\left(\frac{\partial\cos\phi'}{\partial\phi}+i\frac{\partial\sin\phi'}{\partial\phi}\right).\end{aligned}$$

Continuing with the second term, we have

$$\begin{aligned}C_n^mP_n^m\left(\cos(\theta')\right)\left(\cos\phi'+i\sin\phi'\right)^{m-1}\left(\frac{\partial\cos(\phi')}{\partial\theta}+i\frac{\partial\sin(\phi')}{\partial\theta}\right) &=\\ Y_n^m(\theta',\phi')\left(\cos\phi'-i\sin\phi'\right)\left(\frac{\partial\cos(\phi')}{\partial\theta}+i\frac{\partial\sin(\phi')}{\partial\theta}\right)&\end{aligned}$$

and, furthermore,

$$\begin{aligned}\left(\cos\phi'-i\sin\phi'\right)\left(\frac{\partial\cos(\phi')}{\partial\theta}+i\frac{\partial\sin(\phi')}{\partial\theta}\right) &= \cos\phi'\frac{\partial\cos(\phi')}{\partial\theta}+\sin\phi'\frac{\partial\sin(\phi')}{\partial\theta}\\ &+ i\left(\cos\phi'\frac{\partial\sin(\phi')}{\partial\theta}-\sin\phi'\frac{\partial\cos(\phi')}{\partial\theta}\right).\end{aligned}$$

Since

$$\cos\phi'\frac{\partial\cos\phi'}{\partial\theta}+\sin\phi'\frac{\partial\sin\phi'}{\partial\theta}=\frac{\partial}{\partial\theta}\frac{1}{2}\left(\cos^2\phi'+\sin^2\phi'\right)=0$$

and

$$\begin{aligned}\cos\phi'\frac{\partial\sin\phi'}{\partial\theta}-\sin\phi'\frac{\partial\cos\phi'}{\partial\theta} &= \frac{f(\theta,\phi)}{\sqrt{f(\theta,\phi)^2+g(\theta,\phi)^2}}\frac{\partial}{\partial\theta}\left(\frac{g(\theta,\phi)}{\sqrt{f(\theta,\phi)^2+g(\theta,\phi)^2}}\right)\\ &- \frac{g(\theta,\phi)}{\sqrt{f(\theta,\phi)^2+g(\theta,\phi)^2}}\frac{\partial}{\partial\theta}\left(\frac{f(\theta,\phi)}{\sqrt{f(\theta,\phi)^2+g(\theta,\phi)^2}}\right)\\ &= \frac{1}{f(\theta,\phi)^2+g(\theta,\phi)^2}\left(f(\theta,\phi)\frac{\partial}{\partial\theta}g(\theta,\phi)-g(\theta,\phi)\frac{\partial}{\partial\theta}f(\theta,\phi)\right),\end{aligned}$$

we arrive at

$$\begin{aligned}\frac{\partial}{\partial\theta}Y_n^m(\theta',\phi') &= C_n^m\left(P_n^m\right)'\left(\cos\theta'\right)\left(\cos\phi'+i\sin\phi'\right)^m\frac{\partial\cos\theta'}{\partial\theta}+\\ &+ i\,mY_n^m(\theta',\phi')\frac{1}{f(\theta,\phi)^2+g(\theta,\phi)^2}\left(f(\theta,\phi)\frac{\partial}{\partial\theta}g(\theta,\phi)-g(\theta,\phi)\frac{\partial}{\partial\theta}f(\theta,\phi)\right)\end{aligned}$$

and

$$\frac{\partial}{\partial\phi}Y_n^m(\theta',\phi') = C_n^m\left(P_n^m\right)'\left(\cos\theta'\right)\left(\cos\phi'+i\sin\phi'\right)^m\frac{\partial\cos\theta'}{\partial\phi}+$$
$$+\,i\,mY_n^m(\theta',\phi')\frac{1}{f(\theta,\phi)^2+g(\theta,\phi)^2}\left(f(\theta,\phi)\frac{\partial}{\partial\phi}g(\theta,\phi)-g(\theta,\phi)\frac{\partial}{\partial\phi}f(\theta,\phi)\right).$$

We now calculate the factors $\frac{\partial\cos\theta'}{\partial\theta}$, $\frac{\partial\cos\theta'}{\partial\phi}$ and

$$\frac{1}{f(\theta,\phi)^2+g(\theta,\phi)^2}\left(f(\theta,\phi)\frac{\partial}{\partial\theta}g(\theta,\phi)-g(\theta,\phi)\frac{\partial}{\partial\theta}f(\theta,\phi)\right).$$

For the icosahedron group, these factors are of the form

$$\frac{\partial\cos\theta'}{\partial\theta} = \frac{\partial h(\theta,\phi)}{\partial\theta} = \alpha_1\cos\theta\cos\phi+\beta_1\cos\theta\sin\phi+\gamma_1\sin\theta$$
$$\frac{\partial\cos\theta'}{\partial\phi} = \frac{\partial h(\theta,\phi)}{\partial\phi} = \sin\theta\left(A_1\cos\phi+B_1\sin\phi\right)$$
$$f(\theta,\phi)\frac{\partial}{\partial\theta}g(\theta,\phi)-g(\theta,\phi)\frac{\partial}{\partial\theta}f(\theta,\phi) = A_2\cos\phi+B_2\sin\phi$$
$$f(\theta,\phi)\frac{\partial}{\partial\phi}g(\theta,\phi)-g(\theta,\phi)\frac{\partial}{\partial\phi}f(\theta,\phi) = \sin\theta\left(\alpha_2\cos\theta\cos\phi+\beta_2\cos\theta\sin\phi+\gamma_2\sin\theta\right),$$

with the numbers α_1, β_1, γ_1, A_1, B_1, α_2, β_2, γ_2, A_2, B_2 determined by direct computation using e.g. Mathematica^{TM} and then tabulated.

Department of Applied Mathematics, University of Colorado at Boulder, Boulder, CO 80309

ROTATIONALLY INVARIANT QUADRATURES FOR THE SPHERE

CORY AHRENS AND GREGORY BEYLKIN

ONLINE SUPPLEMENT

Coordinates of vertices of an icosahedron. We set $\alpha = \left(1-\sqrt{5}\right)/2$ and list the Cartesian coordinates of the vertices of an icosahedron inscribed into the unit sphere.

Vertex	Coordinate
v_1	$(0,\alpha,1)/\sqrt{1+\alpha^2}$
v_2	$(0,\alpha,-1)/\sqrt{1+\alpha^2}$
v_3	$(1,0,\alpha)/\sqrt{1+\alpha^2}$
v_4	$(1,0,-\alpha)/\sqrt{1+\alpha^2}$
v_5	$(\alpha,1,0)/\sqrt{1+\alpha^2}$
v_6	$(\alpha,-1,0)/\sqrt{1+\alpha^2}$
v_{i+6}	$-v_i$, $i=1\ldots6$

TABLE 1. Cartesian coordinates of an icosahedron. Here $\alpha = \left(1-\sqrt{5}\right)/2$.

Elements of the icosahedral rotation group as quaternions. The action of an element from the icosahedral rotation group may be represented using quaternions. Here we list a quaternionic representation of the icosahedral rotation group.

$\mathbf{q}_1 = -\frac{1}{2} - \mathbf{i}\frac{1}{2} + \mathbf{j}\frac{1}{2} - \mathbf{k}\frac{1}{2}$	$\mathbf{q}_{21} = \mathbf{i}$	$\mathbf{q}_{41} = -\beta + \mathbf{i}\frac{1}{2} + \mathbf{k}\gamma$
$\mathbf{q}_2 = -\frac{1}{2} - \mathbf{i}\frac{1}{2} + \mathbf{j}\frac{1}{2} + \mathbf{k}\frac{1}{2}$	$\mathbf{q}_{22} = -\mathbf{i}\beta - \mathbf{j}\frac{1}{2} - \mathbf{k}\gamma$	$\mathbf{q}_{42} = -\beta + \mathbf{i}\frac{1}{2} - \mathbf{k}\gamma$
$\mathbf{q}_3 = -\frac{1}{2} - \mathbf{j}\beta + \mathbf{k}\gamma$	$\mathbf{q}_{23} = -\mathbf{i}\beta + \mathbf{j}\frac{1}{2} + \mathbf{k}\gamma$	$\mathbf{q}_{43} = -\beta + \mathbf{i}\gamma - \mathbf{j}\frac{1}{2}$
$\mathbf{q}_4 = -\frac{1}{2} + \mathbf{j}\beta + \mathbf{k}\gamma$	$\mathbf{q}_{24} = -\mathbf{i}\beta + \mathbf{j}\frac{1}{2} - \mathbf{k}\gamma$	$\mathbf{q}_{44} = -\beta + \mathbf{i}\gamma + \mathbf{j}\frac{1}{2}$
$\mathbf{q}_5 = -\frac{1}{2} + \mathbf{i}\frac{1}{2} - \mathbf{j}\frac{1}{2} - \mathbf{k}\frac{1}{2}$	$\mathbf{q}_{25} = \mathbf{i}\gamma - \mathbf{j}\beta - \mathbf{k}\frac{1}{2}$	$\mathbf{q}_{45} = -\beta - \mathbf{i}\gamma - \mathbf{j}\frac{1}{2}$
$\mathbf{q}_6 = -\frac{1}{2} + \mathbf{i}\frac{1}{2} - \mathbf{j}\frac{1}{2} + \mathbf{k}\frac{1}{2}$	$\mathbf{q}_{26} = \mathbf{i}\gamma - \mathbf{j}\beta + \mathbf{k}\frac{1}{2}$	$\mathbf{q}_{46} = -\beta - \mathbf{i}\gamma + \mathbf{j}\frac{1}{2}$
$\mathbf{q}_7 = -\frac{1}{2} - \mathbf{i}\beta + \mathbf{j}\gamma$	$\mathbf{q}_{27} = \mathbf{i}\gamma + \mathbf{j}\beta + \mathbf{k}\frac{1}{2}$	$\mathbf{q}_{47} = \gamma - \mathbf{i}\frac{1}{2} - \mathbf{j}\beta$
$\mathbf{q}_8 = -\frac{1}{2} - \mathbf{i}\beta - \mathbf{j}\gamma$	$\mathbf{q}_{28} = -\mathbf{i}\gamma - \mathbf{j}\beta + \mathbf{k}\frac{1}{2}$	$\mathbf{q}_{48} = \gamma - \mathbf{i}\frac{1}{2} + \mathbf{j}\beta$
$\mathbf{q}_9 = -\frac{1}{2} + \mathbf{i}\gamma - \mathbf{k}\beta$	$\mathbf{q}_{29} = \mathbf{i}\beta + \mathbf{j}\frac{1}{2} - \mathbf{k}\gamma$	$\mathbf{q}_{49} = \gamma - \mathbf{j}\frac{1}{2} - \mathbf{k}\beta$
$\mathbf{q}_{10} = -\frac{1}{2} + \mathbf{i}\gamma + \mathbf{k}\beta$	$\mathbf{q}_{30} = \frac{1}{2} - \mathbf{i}\frac{1}{2} - \mathbf{j}\frac{1}{2} - \mathbf{k}\frac{1}{2}$	$\mathbf{q}_{50} = \gamma - \mathbf{j}\frac{1}{2} + \mathbf{k}\beta$
$\mathbf{q}_{11} = -\frac{1}{2} - \mathbf{i}\gamma - \mathbf{k}\beta$	$\mathbf{q}_{31} = \frac{1}{2} - \mathbf{i}\frac{1}{2} - \mathbf{j}\frac{1}{2} + \mathbf{k}\frac{1}{2}$	$\mathbf{q}_{51} = \gamma + \mathbf{i}\beta - \mathbf{k}\frac{1}{2}$
$\mathbf{q}_{12} = -\frac{1}{2} - \mathbf{i}\gamma + \mathbf{k}\beta$	$\mathbf{q}_{32} = \frac{1}{2} - \mathbf{j}\beta + \mathbf{k}\gamma$	$\mathbf{q}_{52} = \gamma + \mathbf{i}\beta + \mathbf{k}\frac{1}{2}$
$\mathbf{q}_{13} = -\frac{1}{2} + \mathbf{i}\beta + \mathbf{j}\gamma$	$\mathbf{q}_{33} = \frac{1}{2} + \mathbf{j}\beta + \mathbf{k}\gamma$	$\mathbf{q}_{53} = -\gamma - \mathbf{i}\frac{1}{2} - \mathbf{j}\beta$
$\mathbf{q}_{14} = -\frac{1}{2} + \mathbf{i}\beta - \mathbf{j}\gamma$	$\mathbf{q}_{34} = \frac{1}{2} + \mathbf{i}\frac{1}{2} + \mathbf{j}\frac{1}{2} - \mathbf{k}\frac{1}{2}$	$\mathbf{q}_{54} = -\gamma - \mathbf{i}\frac{1}{2} + \mathbf{j}\beta$
$\mathbf{q}_{15} = -\mathbf{i}\frac{1}{2} + \mathbf{j}\gamma - \mathbf{k}\beta$	$\mathbf{q}_{35} = \frac{1}{2} + \mathbf{i}\frac{1}{2} + \mathbf{j}\frac{1}{2} + \mathbf{k}\frac{1}{2}$	$\mathbf{q}_{55} = -\gamma - \mathbf{j}\frac{1}{2} - \mathbf{k}\beta$
$\mathbf{q}_{16} = -\mathbf{i}\frac{1}{2} + \mathbf{j}\gamma + \mathbf{k}\beta$	$\mathbf{q}_{36} = 1$	$\mathbf{q}_{56} = -\gamma - \mathbf{j}\frac{1}{2} + \mathbf{k}\beta$
$\mathbf{q}_{17} = -\mathbf{i}\frac{1}{2} - \mathbf{j}\gamma + \mathbf{k}\beta$	$\mathbf{q}_{37} = -\beta + \mathbf{j}\gamma - \mathbf{k}\frac{1}{2}$	$\mathbf{q}_{57} = -\gamma + \mathbf{i}\beta - \mathbf{k}\frac{1}{2}$
$\mathbf{q}_{18} = -\mathbf{j}$	$\mathbf{q}_{38} = -\beta + \mathbf{j}\gamma + \mathbf{k}\frac{1}{2}$	$\mathbf{q}_{58} = -\gamma + \mathbf{i}\beta + \mathbf{k}\frac{1}{2}$
$\mathbf{q}_{19} = \mathbf{k}$	$\mathbf{q}_{39} = -\beta - \mathbf{j}\gamma - \mathbf{k}\frac{1}{2}$	$\mathbf{q}_{59} = \beta + \mathbf{i}\frac{1}{2} + \mathbf{k}\gamma$
$\mathbf{q}_{20} = \mathbf{i}\frac{1}{2} + \mathbf{j}\gamma + \mathbf{k}\beta$	$\mathbf{q}_{40} = -\beta - \mathbf{j}\gamma + \mathbf{k}\frac{1}{2}$	$\mathbf{q}_{60} = \beta + \mathbf{i}\frac{1}{2} - \mathbf{k}\gamma$

TABLE 2. Quaternionic representation of the icosahedral rotation group. Here we set $\beta = \frac{1+\sqrt{5}}{4}$ and $\gamma = \frac{1-\sqrt{5}}{4}$.

DEPARTMENT OF APPLIED MATHEMATICS, UNIVERSITY OF COLORADO AT BOULDER, BOULDER, CO 80309